Synthesis and Temperature-dependent Phase Behavior of a Dendritic Dipeptide

Emma Yeung

Abstract

Liquid crystals (LCs) are a unique class of molecules that combine the fluidity of a liquid and the molecular order of a solid. Dendrons, which are a class of polymers with liquid crystalline properties, are often grafted onto peptides to create hybrids with the ability to withstand hostile environments in the LC phase and great potential for applications in medicine, energy, and nanotechnology. While individual peptide-dendron hybrids can be manipulated for their structure and function, the resulting hydrogen bonding and London dispersion forces (LDFs) can determine whether and when an LC forms. To further investigate the effects of electrostatic forces on LC formation in hybrids with short dendrons, a novel dendritic lysine-alanine dipeptide was synthesized and characterized. A leaving group was attached to a dendritic benzamide through esterification in order to ensure the successful attachment of lysine to the dendron. After attaching the dendron to lysine through a trans-amidation reaction, alanine was grafted onto the dendron-lysine through a peptide-coupling reaction, and the final product was confirmed through ^{1}H NMR. Polarized optical microscopy (POM) and differential scanning calorimetry (DSC) experiments revealed that isotropization from the solid phase occurred at 102°C. An additional peak at a lower temperature was seen in the DSC data, but the lack of fluidity during POM experiments led to inconclusive results regarding LC phase formation. Data from previous studies suggested that extensive hydrogen bonding may prevent an LC phase formation; however, an attempt to minimize potential hydrogen bonding sites in this experiment did not result in an LC phase, suggesting that the appropriate balance between LDFs from the dendrons and H-bonding in the peptide has not been achieved.

Introduction

The liquid crystal (LC) mesophase is an intermediate phase that may be formed between the solid and liquid phase. LCs are formed from interactions between mesogenic groups that induce liquid crystalline properties: the combination of a rigid component that aligns the molecule in one direction and a flexible component that hinders crystallization (Tschierske, 2012). This allows for the ability to maintain molecular order like a solid but flow like a liquid. Because mesogenic groups maintain orientation and allow for molecular flexibility, the LC phase not only preserves functionality but also allows for control of molecular structure (Saez et al., 2005). LCs have been utilized in electronic devices — known as liquid crystal displays (LCDs) — at room temperature, but they also show potential in biological contexts (Sharma et al., 2017).

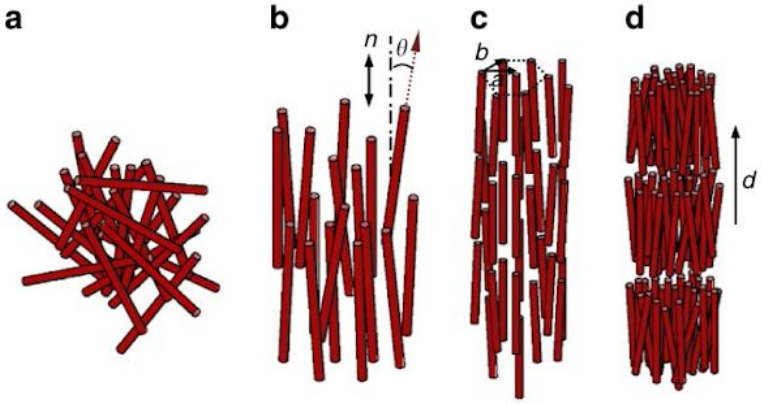

Figure 1. Schematic representations of an isotropic liquid **(a)** and varying liquid crystals based on their packing densities **(b, c, d)**. Regardless of density, all liquid crystals maintain molecular orientation and shape (Paineau et al., 2001).

In particular, there is an ongoing investigation into the LC properties of dendrimers as biomaterials (Kuang et al., 2011). Dendrimers are macromolecules consisting of a series of hydrocarbon branches extending from an inner core (Fig 2) (Crespo et al., 2005). Synthesized by attaching repeated units of dendrons in an outwards direction at branching points, called generations (Zeng et al., 1997), dendrimers have three distinct sections: a core, branches, and branching units that link the two (Sadler et al., 2005). Due to their extensively branched spherical structure (Nanjwade et al., 2009), dendrons, which are sections of a dendrimer with a focal point (Fig 2), have unique properties compared to linear polymers (Sadler et al., 2005), including the

ability to withstand temperature and pH change, resist deformation, and self-assemble. In order to self-assemble and rapidly form large nanostructures (Hudson et al., 1997), dendrons must be in the LC phase (Mendes et al., 2017), requiring them to be composed of mesogens. The rigid mesogens, usually phenyl groups, are held together by flexible alkyl groups (Ponomarenko et al., 2001), and varying the organization of mesogenic groups, such as altering hydrocarbon length, will alter the properties of the LC phase (Percec et al., 2007).

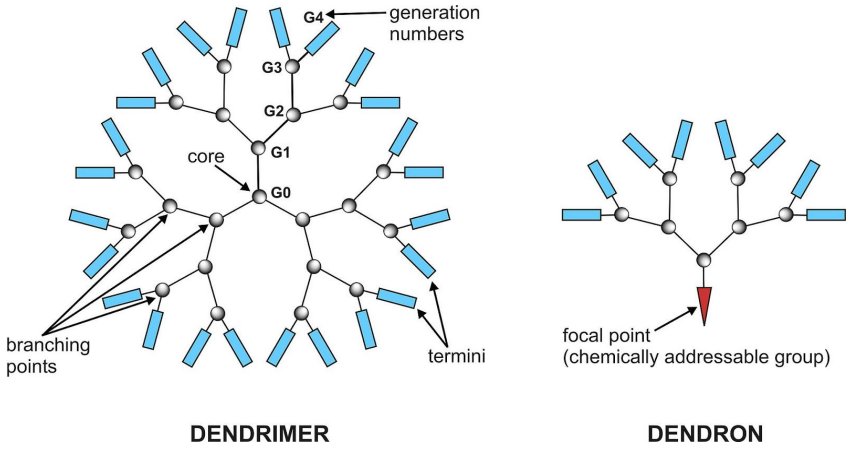

Figure 2. Schematic representation of a dendrimer and a dendron (Nanjwade et al., 2009).

Because dendrons have high cytotoxicity and poor solubility in polar solvents (Duncan et al., 2005), grafting peptides on dendrons at their focal point combines the liquid crystalline properties of dendrons with the versatile functionality of peptides as catalysts, transmembrane channels, and therapeutics (Barkley et al., 2018). In the LC phase, individual hybrids take on a wedge shaped conformation and self-assemble into columns held together by intermolecular forces (Barkley et al., 2017). The hydrophilic peptides are hidden within the column and held together by hydrogen bonding (Barkley et al., 2018), while the hydrophobic dendrites are located on the periphery and held together by π-stacking of the aromatic rings and Van der Waals attractions of the alkyl chains (Fig 3) (Rosen et al., 2011).

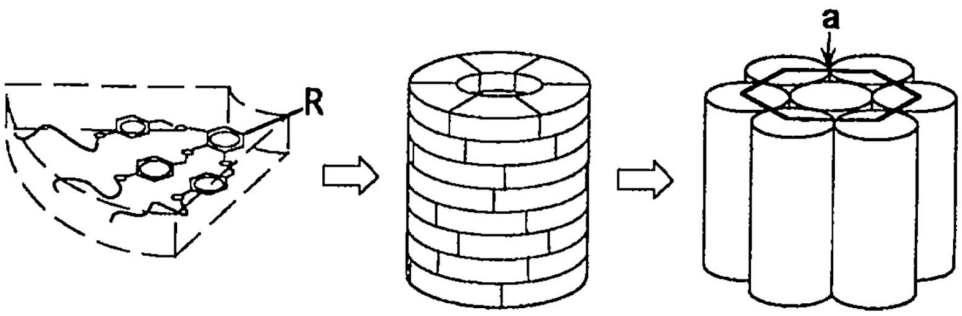

Figure 3. Model of the wedge shaped peptide-dendron hybrid, the 3D lattice of the self-assembled columnar structure, and the columns in a hexagonal columnar phase (Hudson et al., 1997).

Similar to proteins (Percec et al., 2004), peptide-dendron hybrid structure and function are heavily affected by all levels of hierarchy, starting at individual hybrids. For example, changes in amino acid sequences is expected to result in changes in structure and properties in the hybrid (Marine et al., 2015). Barkley et al. (2017 and 2018) rearranged an amino acid sequence in a peptide-dendron hybrid consisting of lysine and leucine from a fourteen amino acid (Leu-Ly-Ly-Leu) pattern to a seven amino acid (Ly-Leu-Ly-Leu) pattern (Fig 4). The former organized into an alpha-helical secondary structure, while the latter organized into a beta-sheeted secondary structure. The ability to alter amino acids and dendrons allows the structures to be optimized for various applications, allowing the hybrids to serve as porous protein channel mimics (Marine et al., 2016), transmembrane channels (Percec et al., 2005), and drug delivery vehicles (Sadler et al., 2005).

(a)

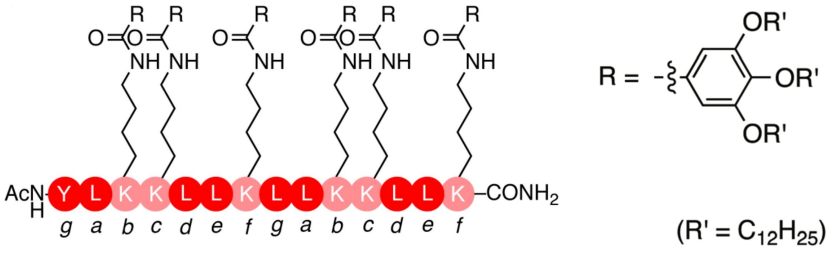

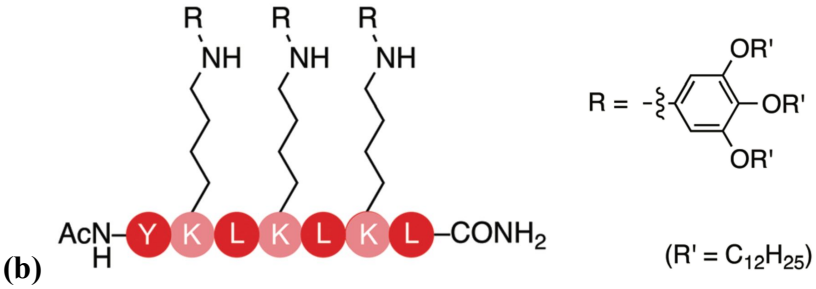

(b)

Figure 4. Scheme of the α-helical bundle forming dendron-peptide hybrid **(a)** and the β-sheet forming dendron-peptide hybrid **(b)**. (Y=Tyrosine; K=Lysine; L=Leucine)

The ultimate goal of synthesizing variations of peptide-dendron hybrids is to create hybrids with short dendrons that exist as LCs at room temperature. While short dendrons are preferable in biological contexts, LC hybrids are most effective at room temperature (Sharma et al., 2017). Pecec et al (2006) designed and synthesized a peptide-dendron hybrid with a generation two (G2) dendron with an LC phase between 55℃ and 97℃, reaching a balance between hydrogen bonding and London dispersion forces. However, peptide-dendron hybrids face several limitations regarding liquid crystal formation and self-assembly. Inability to enter the LC phase or to self-assemble, a property of the LC phase, will hinder the hybrid's functionality. Several hybrids have entered the isotropic phase directly from the crystalline phase (Barkley et al., 2018; Gao et al., 2011), and their alkyl chains underwent crystallization (Barkley et al., 2017). It was suspected to be an excessive amount of H-bonding that overpowered London dispersion forces. Mostly in hybrids with small dendrons, the presence of too many hydrogen bonds creates strong electrostatic forces, causing the molecule to favor crystallization (Mendes et al., 2017). This project designed and synthesized a dendritic dipeptide with lysine, alanine, and nonpolar protective groups (t-BOC and OMe) in order to further explore the desired characteristics of peptide-dendron hybrids.

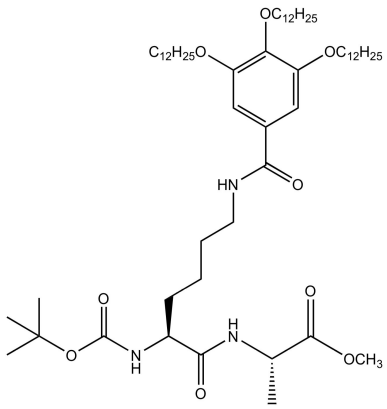

Figure 5. Structure of the dendritic dipeptide drawn on ChemDraw.

Materials and Methods

Materials and Techniques

Anhydrous tetrahydrofuran (THF, 99.9%), anhydrous dichloromethane (DCM, 98%), pentafluorophenol (99%), N,N-diisopropylethylamine (DIEA), N,N'-dicyclohexylcarbodiimide (DCC, 99%), N-(3-Dimethylaminopropyl)-N′-ethylcarbodiimide hydrochloride (EDC-HCL, >98%), 4-(Dimethylamino)pyridine (DMAP, ≥99%), magnesium sulfate drying agent (MgSO4, >98%), and potassium carbonate (K2CO3, 99.9%) were used as received from Aldrich. A.C.S. Reagent-grade (>95%) dichloromethane and anhydrous N,N-dimethylformamide (DMF), were used as received from EMD Millipore. Acetonitrile (CH3CN) and acetone (A.C.S. grade, >99.5%) were used as received from Fisher. Methanol (MeOH, A.C.S. reagent) and tetrahydrofuran (THF, A.C.S. reagent) were used as received from BDH Chemicals. Chloroform-d with 0.03% v/v tetramethylsilane (CDCl3, 99.8% D) was used as received from Cambridge Isotope Laboratories. Methyl 3,4,5-trihydroxybenzoate (98%) was used as received from Aldrich. 4-(N,N-dimethylamino)pyridinium tosylate (DPTS) was taken from laboratory stock synthesized by others according to literature procedures (Barkley et al., 2018).

Thin layer chromatography (TLC) was performed on 60 Å silica gel plates (250 μm, Whatman) and observed using a UV lamp (254 nm). Flash column chromatography was performed on a Teledyne Isco CombiFlash Rf with RediSep Rf Normal Phase disposable silica cartridges. ^{1}H NMR spectra were recorded on a Bruker NanoBay (^{1}H, 400 MHz) instrument or a

Bruker AVANCE III instrument equipped with a Prodigy cold probe (^{1}H, 500 MHz). Chemical shift values are referenced to the residual proton solvent peaks (^{1}H: CDCl3), in which the analyte is dissolved.

Polarized optical microscopy (POM) was performed on an Olympus BX43 optical microscope with a FP82HT hot stage and FP900 controller (both from Mettler Toledo). An Infinity 2 camera and Lumenera Infinity Analyze software were used to acquire micrographs.

Differential scanning microscopy (DSC) was performed on a DSC Q2000 from TA Instruments.

Reaction Scheme

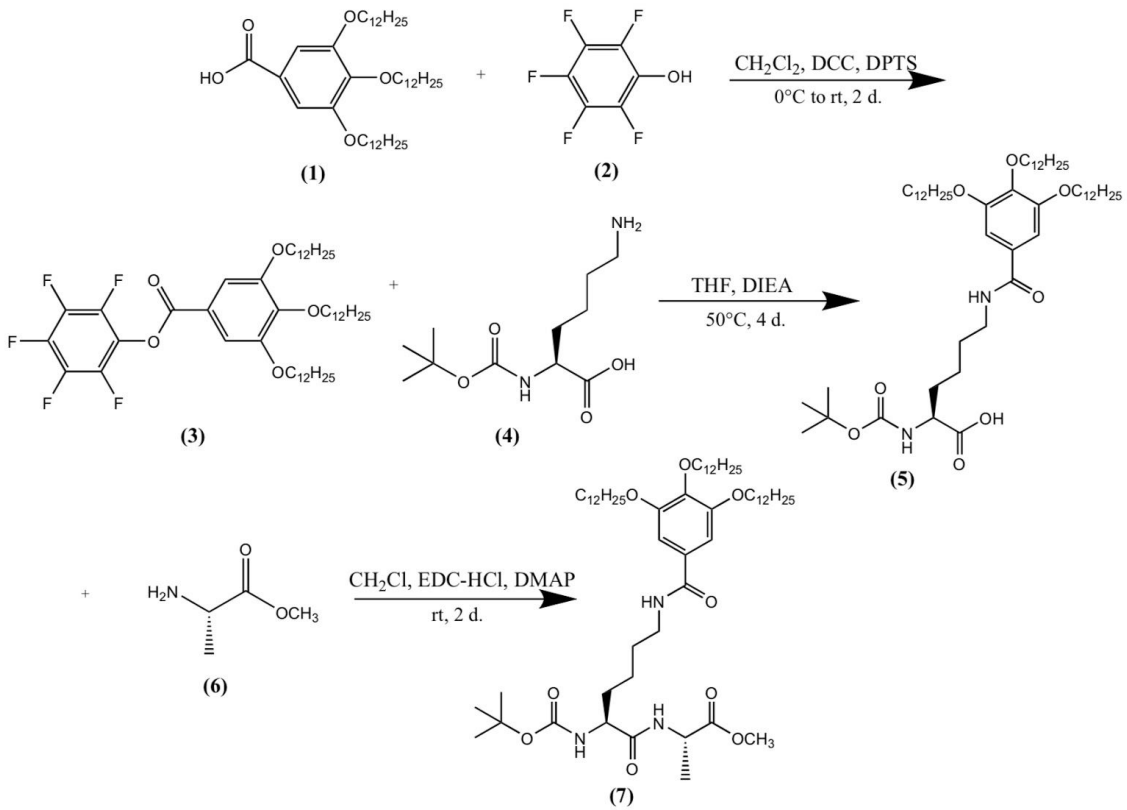

Figure 6. Reaction scheme of the peptide-dendron synthesis was drawn through ChemDraw.

Esterification of the Dendritic Benzoic Acid (3)

In a 10 mL round bottom flask (RBF), the benzoic acid (1) (995mg, 1.47 mmol) and the pentafluorophenol (2) (325.2mg, 1.77 mmol) were dissolved in DCM (3 mL). Before placing the RBF in an ice water bath, DPTS (234.6mg, 0.797 mmol) was put in the DCM solution. Drop by drop, DCC (363.5mg, 1.76 mmol) was injected into the RBF. After all the DCC had been added, the RBF was put at room temperature. The solution in the RBF was left to stir for two days. With DCM as the solvent, a TLC was done of the crude sample in order to confirm that a reaction occurred. Before vacuum filtration was done to remove the solid impurities, the solution in the RBF was transferred into a large erlenmeyer flask. Column chromatography was run at 100% DCM, and the first peak was collected and used. The solvent collected was removed with rotary evaporation. Recrystallization occurred when the flask was left in the fridge overnight. Reaction success was confirmed through ^{1}H NMR, and a TLC was done of the purified sample (R_f=0.923).

Trans-amidation of the Pentafluorophenyl Ester (5)

In a 25 mL RBF, the pentafluorophenyl ester (391.6mg, 0.466 mmol) was dissolved in THF (12 mL). Then, the Nα-Boc-$_L$-Lysine (127.0mg, 0.520 mmol) and the DIEA (120µL, 0.713 mmol) were added to the THF solution. The RBF was attached to a reflux condenser, clamped to a ring stand, and lowered into an oil bath located above a hot plate set at 55 °C. The reaction was run for 4 days. After a TLC of the crude was done to confirm that the reaction occurred, THF was removed from the solution by rotary evaporation, which resulted in a solid precipitate. DCM was used to dissolve the solid precipitate, and deionized water was added to the DCM solution. After the water and DCM layer showed clear distinction, the organic DCM layer was extracted. This process was repeated once with deionized water and once with a saturated NaCl solution (brine). $MgSO_4$, a drying agent, was used to remove any remaining aqueous components in the DCM layer, and the $MgSO_4$ was removed via vacuum filtration. Column chromatography was run with a gradient of 100% DCM to 90% DCM/10% MeOH. The collected peaks were rotovapped, and recrystallization happened after the test tube was left overnight. Reaction success was confirmed through ^{1}H NMR, and a TLC was done of the purified sample (R_f=0.442).

Coupling of $_L$-Alanine (7)

In a 10 mL RBF, the dendritic lysine (272.8mg, 0.302 mmol) was dissolved in DCM (4 mL). $_L$-Alanine (34.6mg, 0.336 mmol), EDC-HCl (72.7mg, 0.379 mmol), and DMAP (64.7mg, 0.530 mmol) were added to the RBF. The DCM solution was left at room temperature for two days. A TLC was done to confirm the occurrence of the reaction. A 10% v/v acetic acid solution was added to the RBF. After the acetic acid and DCM layer showed clear distinction, the organic DCM layer was extracted. This process was repeated once with a saturated sodium bicarbonate ($NaHCO_3$) solution, once with deionized water, and once with brine. $MgSO_4$ removed the remaining aqueous components in the DCM layer, and the $MgSO_4$ was removed via vacuum filtration. Column chromatography was run with a gradient of 100% DCM to 95% DCM/5% MeOH to 90% DCM/10% MeOH. Reaction success was confirmed through ^{1}H NMR, and a TLC was done of the purified sample (R_f=0.667).

Results

A novel dendritic dipeptide consisting of lysine and alanine was synthesized through an esterification, a trans-amidation, and a peptide-coupling reaction. Through thin layer chromatography (TLC), the reaction was tested for completion and purity. Before purification, the crude product and starting material were ran on the TLC for comparison. Different spots for the crude and the starting material on the TLC indicated that a reaction had occurred. Purification was considered complete when the product showed one clear spot. ^{1}H NMR was used to ensure the correct molecule had been synthesized and to determine purity. All NMR spectra was done in deuterated chloroform (chloroform-D), which has a chemical shift of 7.37. The baseline of all ^{1}H NMR integrals was set at 9 for the three nonpolar methyl groups at the end of each dendron. The nine hydrogens have the lowest chemical shift value due to their electropositive location at the end of the hydrocarbon chain.

Esterification of the Dendritic Benzoic Acid (3)

The purpose of esterifying the dendritic benzoic acid was to create an intermediate to attach the dendron to the amino acid. (3) was synthesized with a yield of 80.1% (997mg,

1.19mmol) through a DCC esterification. DCC was the dehydrating agent, while DPTS acted as the catalyst. After synthesis, a ^{1}H NMR and a ^{19}F NMR were taken to confirm reaction completion and purity.

In the ^{1}H NMR of (3), a peak at the chemical shift value of ~4.07 represents the six hydrogens next the electronegative oxygens. The electronegativity causes the protons on the nearby hydrogens to be deshielded, shifting the hydrogen peaks downfield. Due to the inductive effect, there is a peak at ~1.52, signifying the next six hydrogens located two carbons from the oxygen. Typical of most cyclic hydrogens, the hydrogens on the phenol ring have a shift of ~7.39. Additionally, the ^{19}F NMR spectra confirmed the structure of pentafluorophenol. The ^{1}H NMR and ^{19}F NMR spectra of the pure product was compared to the spectra of the product previously synthesized in Barkley (2017).

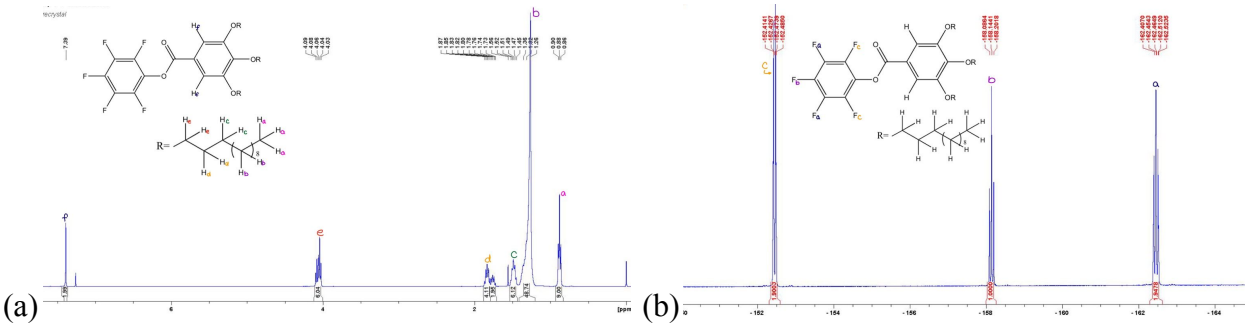

Figure 7. ^{1}H NMR (a) and ^{19}F NMR (b) data for the pentafluorophenyl ester. Each hydrogen in (a) and each fluorine in (b) is labelled to its corresponding peak based on letter.

Trans-amidation of the Pentafluorophenyl Ester (5)

By removing the pentafluorophenol and converting the ester into an amide, the dendron was grafted onto the $_{L}$-lysine sidechain. (5) was synthesized with a yield of 92% (391mg, 0.433mmol) through a trans-amidation. DIEA, a basic salt, was placed in the reaction mixture as a reagent. After synthesis, a ^{1}H NMR was taken and analyzed.

In the ^{1}H NMR of (5), the confirmation of the trans-amidation was seen at the amide group between the dendron and lysine, which has a chemical shift of ~6.60. The hydrogen at the N-terminus of $_{L}$-lysine has a shift of ~5.30. The peak at ~1.45 includes the chemical shifts of the six hydrogens on the BOC protecting group. Due to ionization in chloroform-d, the hydrogen on the carboxylic acid does not show up on the NMR spectra.

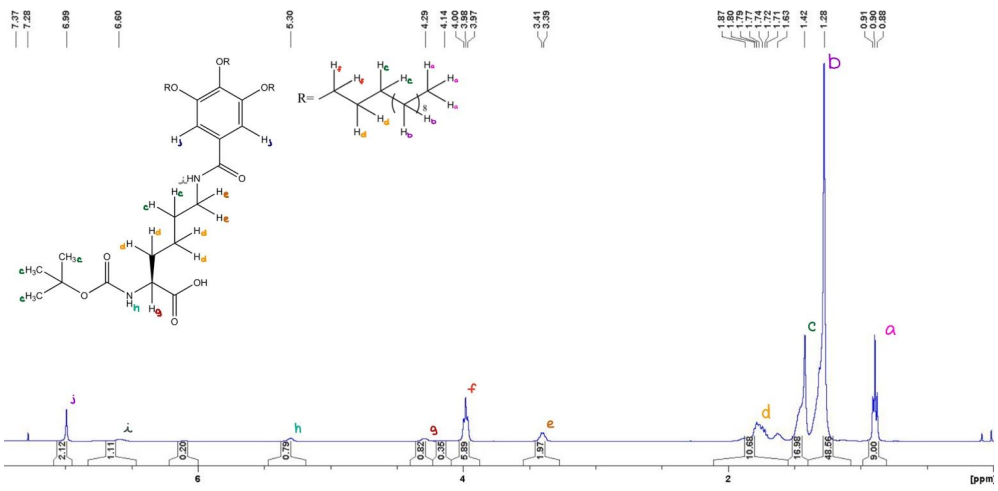

Figure 8. [1]H NMR data of the dendritic lysine. Each hydrogen is labelled to its corresponding peak based on letter. The location of the hydrogens was confirmed through 2D NMR (COSY, HSQC, and HMBC).

Coupling of $_L$-Alanine (7)

(7) was synthesized with a yield of 55% (164mg, 0.166mmol) through EDC coupling. Similar to DCC, EDC-HCl is a dehydrating agent, and DMAP prevented racemerization in the amino acids during the reaction. A [1]H NMR was taken of the purified product.

In the [1]H NMR of (7), there was a chemical shift at ~3.71, representing the three hydrogens in the oxymethyl group attached to C-terminus of $_L$-alanine. The hydrogen at the reaction site, where the N-terminus of $_L$-alanine was attached to the C-terminus of $_L$-lysine, has a chemical shift of ~6.42.

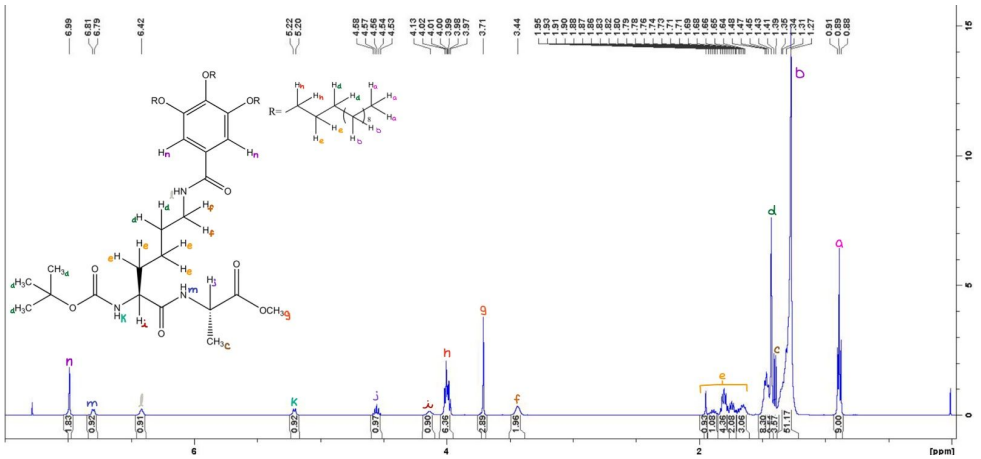

Figure 9. ^{1}H NMR data for the dendritic dipeptide. Each hydrogen is labelled to its corresponding peak based on letter. The location of the hydrogens was confirmed through 2D NMR (COSY, HSQC, and HMBC).

Characterization of the Dendritic Dipeptide

Under the polarized optical microscope (POM), the peptide-dendron hybrid was heated and cooled from 25°C to 120°C at a rate of 5°C/minute. In the solid and LC phase, molecules have special optical anisotropic properties that allow for the refraction of polarized light, called birefringence. Refracting light, the ordered solid and LC phases will exhibit bright colors, whereas the disordered anisotropic liquid will be dark due to the lack of birefringence. Areas lacking the presence of the sample in the solid or liquid crystalline phase will also be dark. To test for liquid crystalline properties, a shear test is performed on the sample. Shearing involves an attempt to move coverslip to determine the fluidity of the sample.

In Fig. 10, the hybrid can be seen as a crystal at 96.8°C. At 98.6°C, the shear test was done, but there was no movement of the coverslip, suggesting the lack of a liquid crystalline phase. This also revealed that the image at 96.8°C is in the crystalline phase, rather than the LC phase. A picture after the test (top right) was taken after the shear test. Around 103°C, the sample entered the isotropic liquid phase, which was indicated by the lack of light. As the sample was cooled, it gradually recrystallized and the properties of birefringence returned, as seen at 85.1°C (bottom right).

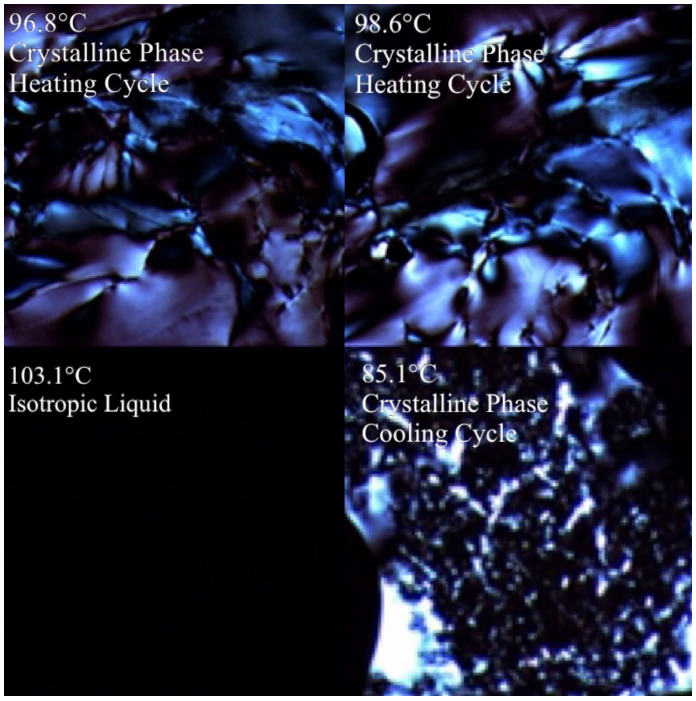

Figure 10. POM images of the dendritic dipeptide taken at various temperatures under cross polarized light and 50x magnification (top left: 96.8°C, top right: 98.6°C; bottom left: 103.1°C, bottom right: 85.1°C)

Differential scanning calorimetry (DSC) experiments showed the phase changes the molecule experienced during heating and cooling. A sample of the dendritic dipeptide and a reference were heated simultaneously from 0°C to 120°C, and the difference in the heat required to increase or the heat released to decrease the temperature between the hybrid and the reference was measured. The hybrid was heated twice and cooled once. During both heating curves, there is a peak at 102°C, indicating a phase change into an isotropic liquid, and during the cooling curve, there is a peak at 95°C, indicating a phase change back into a crystal. Additionally, there is a slight peak at 87°C on both heating curves, which could show a phase transition within the solid state or a phase change into the LC phase.

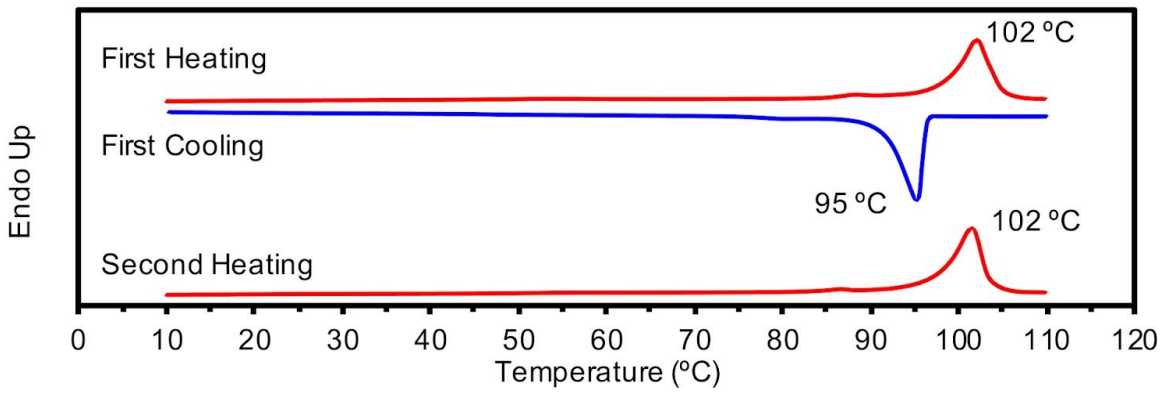

Figure 11. DSC graph of the dendritic dipeptide.

Discussion

Design Rationale

A dendritic dipeptide was recently synthesized in the lab (Fig 12). With an acetyl and an amide protecting group, the dendritic dipeptide composed of lysine and leucine entered the liquid crystal phase at 180°C and the isotropic phase at 210°C. Because LCs are most effective around room temperature (Sharma et al., 2017), structural changes were made in order to lower the temperature of the phase changes.

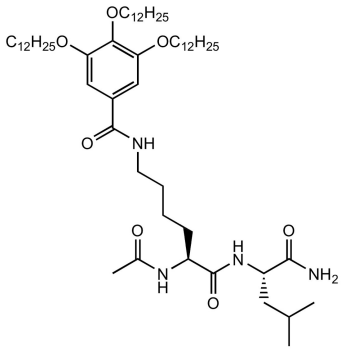

Figure 12. The dendritic dipeptide shown above was previously synthesized in the lab.

Alanine was chosen as a replacement for leucine due to its previous success forming liquid crystalline phases at lower temperatures. With tyrosine as the connector between the peptide and dendron, two variations of generation two (G2) dendritic dipeptides with liquid

crystalline phases were synthesized: one with leucine and one with alanine (Percec et al., 2007). The first entered the LC phase at 71°C and the isotropic phase at 107°C, whereas the latter entered the LC phase at 53°C and the isotropic phase at 96°C. The lower phase change and longer LC phase of alanine were attributed to its lower molar mass (Percec et al., 2007). This led to the hypothesis that lysine and alanine would enter the LC at a lower temperature than lysine and leucine.

To reduce hydrogen bonding sites within the peptide core, an oxymethyl group was added at the C-terminus of alanine, and a t-BOC group was added to the N-terminus of lysine. In the presence of hydrogen bonding sites on other hybrids, t-BOC groups form longer, thus weaker, hydrogen bonds than acetyl (Percec et al., 2005) and amide groups (Barkley et al., 2018).

Synthesis of the Dendritic Dipeptide

The dendritic dipeptide was successfully synthesized in a three step process: an esterification, a trans-amidation, and a peptide-coupling reaction. ^{1}H NMR was used to confirm the existence of the final product. Through POM and DSC experiments, one distinguishable phase transition was identified at 102°C during heating and 95°C during cooling; both of which were presumed to be the transition from solid to isotropic phase. The lower crystallization temperature is due to the slower recrystallization rate of alanine as a substituent (Percec et al., 2007). However, there is a small peak at 87°C, suggesting an additional phase change that could either be a solid-solid or a solid-LC change. Because no fluidity indicating the presence of a liquid crystal was observed, wide angle x-ray scattering (WAXS) experiments are needed to confirm and identify the phase change. If the peak indicates the formation of an LC phase, the switch from leucine to alanine as the second amino acid and the addition of a t-BOC and an oxymethyl protecting group would have successfully decreased the LC phase change by a significant amount from the previously synthesized dendritic dipeptide (Fig 12). The dendritic dipeptide synthesized in this experiment already decreased the isotropization temperature by 107°C.

Analysis of the Liquid Crystalline Phase

Peptide-dendron hybrids with long dendrons have been successful in forming LCs at room temperature due to the control that mesogenic groups within the dendrons offer. The mesogenic groups, consisting of phenol rings and alkyl chains, allow for a balance between molecular order and fluidity. Long hydrocarbon chains reduce the rigid binding of the phenol rings, allowing for thermostability in the LC phase (Ponomarenko et al., 2001). A high density of the peripheral alkyl chains lowers the transition temperature into the LC phase, whereas a high number of aromatic groups raises the isotropization temperature (Barkley et al., 2017). However, hybrids with shorter dendrons are more desirable in biological contexts (Duncan et al., 2005). Due to slow biodegradation, large dendrons result in cellular accumulation (Bolu et al., 2018) and cytotoxicity (Li et al., 2016).

The necessity for short dendrons has shifted emphasis onto the role of hydrogen bonding on the LC phase. Most notably, aromatic carboxylic acids are the earliest dendrons found to have entered the LC phase due to H-bonding and London dispersion forces (LDFs) (Paleos et al., 2001). Considered the strongest electrostatic force, hydrogen bonding is between hydrogen and an electronegative element in the amide and the carboxylic acid groups of peptides, while LDFs are temporary dipoles formed between nonpolar components of the dendrons. The carbonyl-NH hydrogen bonding between peptide backbones encourages intermolecular association, uniting individual peptide-dendron hybrids and promoting self-assembly in the LC phase (Crespo et al., 2005). Gao et al. (2011) investigated the role of hydrogen bonding in hybrids with short dendrons. Polyaspartic acid was attached to progressively longer dendron chains (Fig 13). G1 having the smallest dendron and G3 having the largest dendron, the G1 and G2 molecule did not have an LC mesophase, whereas the G3 molecule did. Additionally, the G3 hybrid entered the LC phase at 40°C and the isotropic phase at 145°C, with the high isotropic phase change attributed to the hydrogen bonding acting as reinforcement in the LC phase. While electrostatic forces are essential to self-assembly, which occurs in the LC phase, strong electrostatic forces cause molecules to favor the crystalline phase (Mendes et al., 2017). Shorter dendrons minimize the distance between polar peptide chains, strengthening the hydrogen bonds between peptide-dendron hybrid columns. By creating a polar dipole, the electrostatic forces cause the

columns to pack, therefore favoring crystallization, limiting mobility, and eliminating the LC phase.

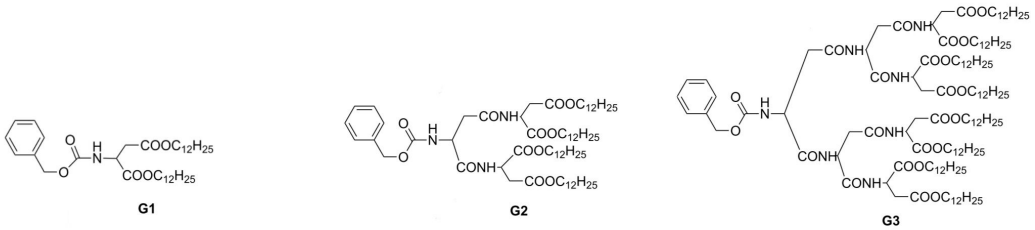

Figure 13. Polyaspartic acid was attached to varying generations of dendrons (Gao et al., 2011).

Therefore, it is crucial to find the balance between H-bonding and London dispersion forces in peptide-dendron hybrids with short dendrons. Percec et al (2005) synthesized a G2 dendron with alanine and tyrosine (Fig 14a) that existed as a LC between 85 and 97°C. Later, in 2006, Percec et al removed two benzyl esters and their peripheral alkyl chains from the same G2 hybrid (Fig 14b), lowering the LC transition temperature to 55°C. Increasing the role of hydrogen bonding, the removal of parts within the dendron decreased the LC transition temperature, demonstrating the ability to favorably manipulate hybrid properties by shifting the role of certain electrostatic forces.

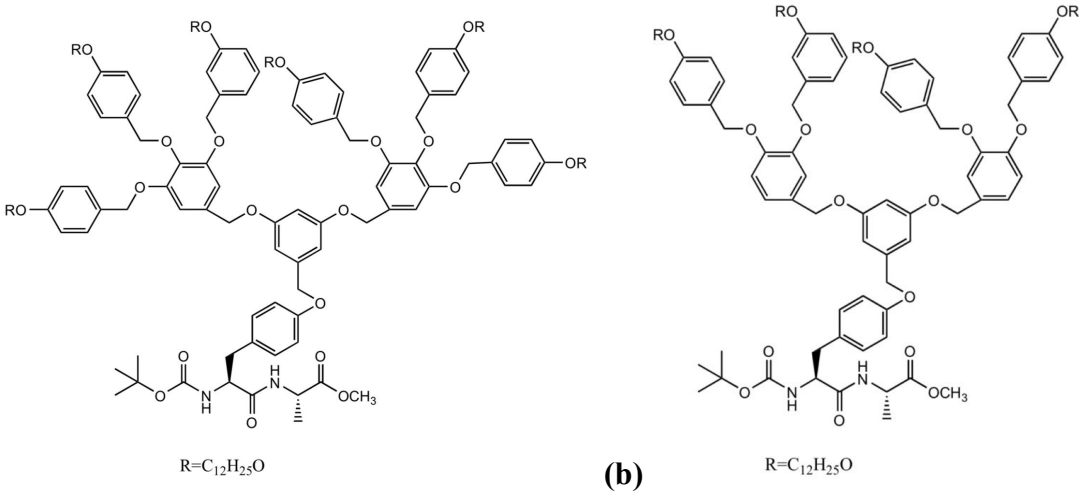

(a) **(b)**

Figure 14. Tyrosine and alanine were grafted onto second generation dendrons. **(a)** is from Percec et al (2005) and **(b)** is from Percec et al (2006).

More work is necessary to gain more insight into the role of hydrogen bonding in LCs to reduce the LC phase transition temperature. Unlike the peptide-dendron hybrids reviewed above (Fig 14b), the dendritic dipeptide synthesized in this experiment has a significantly shorter dendron. The change from tyrosine to lysine also decreased π-stacking in the hybrid. Despite differences in the dendrons, both molecules had similar isotropization temperatures, which could be attributed to their identical peripheral alkyl chains ($C_{12}H_{25}O$). Increasing the length of the peripheral alkyl chains increases favorability into the crystalline phase due to packing (Barkley et al., 2017), suggesting that shorter alkyl chains may raise the melting point of the hybrid.

DSC data indicated an additional phase change at 87°C, but POM experiments did not show any fluidity in the molecule below isotropization temperature. WAXS experiments are necessary to confirm the type of phase change. If the hybrid does, in fact, become a LC at 87°C, it has a small temperature range of fifteen degrees and enters the LC phase at a temperature too high for the LC to be effective. Although isotropization and LC phase change temperatures of this dendritic dipeptide were decreased from the previously synthesized denditic dipeptide (Fig 10), further structural changes must be made to have a definitive LC phase and lower the temperature of the phase change. The lack of an LC phase hinders the ability to draw firm conclusions about the effects of the structural differences and electrostatic forces within this dendritic dipeptide.

Applications

The well-defined architecture, highly organized structure, and good biocompatibility make peptide-dendron hybrids good candidates for functional material, such as synthetic water channels (Kaucher et al., 2007) and catalysts as water-soluble enzymes (Marine et al., 2016). In particular, peptide-dendron hybrids show potential as drug delivery vehicles (Li et al., 2016). Drugs are grafted onto the peptide core and encapsulated within the self-assembling hybrids, with the structure's liquid crystalline properties offering protection from acidic gastrointestinal conditions and limiting drug release (Duncan et al., 2005). Limiting drug release results in a reduction of drug toxicity. Due to the slow biodegradation and cytotoxicity of large dendrons, short phenylic dendrons that do not ionize are preferable (Duncan et al., 2005). The high cost and

energy needed to manufacture the peptide-dendron hybrids pose another obstacle that prevents hybrids from being widely used (Lee et al., 2016). The ability to withstand a wide range of environments in the liquid crystalline phase (Li et al., 2016) makes peptide-dendron hybrids with short dendrons, similar to the hybrid synthesized in this experiment, to be highly favored as a potential drug delivery vehicle.

Conclusion and Future Research:

A novel dendritic dipeptide with a short dendron was synthesized with lysine and alanine acting as the amino acids and BOC and oxymethyl acting as nonpolar protective groups on the amino acids. One definitive phase transition into isotropic phase at 102 °C and into the crystalline phase at 95°C was identified. Additionally, the presence of small peak at 87°C in both heating and cooling curves that suggests the possibility of an additional phase change. However, the sample did not exhibit fluidity during POM experiments, rendering the data inconclusive. Wide angle X-ray scattering experiments are needed to confirm or deny the existence of the LC phase. The insufficient evidence from POM and DSC experiments led to the inability to perform WAXS experiments. If the hybrid is confirmed to enter the LC phase at 87°C, the LC would have a relatively small range and enter the phase at a temperature higher than room temperature. Because small structural changes determine crucial properties, like the ability to form an LC and phase change temperatures, careful planning is needed to design the ideal hybrid with a balance of hydrogen bonding and London dispersion forces necessary for an LC with a wide temperature range occurring at room temperature. In the future, the stability and longevity of peptide-dendron hybrids should be tested in numerous biological environments, including the human body.

References

Barkley, D. A., Rokhlenko, Y., Marine, J. E., David, R., Sahoo, D., Watson, M. D., Koga, T., Osuji, C., O., Rudick, J., G. (2017). Hexagonally Ordered Arrays of α-Helical Bundles Formed from Peptide-Dendron Hybrids. Journal of the American Chemical Society, 139(44), 15977-15983. doi:10.1021/jacs.7b09737

Barkley, D. A., Han, S. U., Koga, T., Rudick, J. G. (2018). Peptide–dendron Hybrids That Adopt Sequence-encoded β-sheet Conformations. Polymer Chemistry,9(40), 4994-5001. doi:10.1039/c8py00882e

Bolu, B. S., Sanyal, R., Sanyal, A. (2018) Drug Delivery Systems from Self-Assembly of Dendron-Polymer Conjugates. Molecules, 23, 1570. doi:10.3390/molecules23071570

Crespo, L., Sanclimens, G., Pons, M., Giralt, E., Royo, M., Albericio, F. (2005). Peptide and Amide Bond-Containing Dendrimers. Chemical Review, 105, 1663-1681. doi:10.1021/cr030449l

Duncan, R., Izzo, L. (2005). Dendrimer Biocompatibility and Toxicity. Advanced Drug Delivery Reviews,57(15), 2215-2237. doi:10.1016/j.addr.2005.09.019

Gao, B., Li, H., Xia, D., Sun, S., Ba, X. (2011). Amphiphilic Dendritic Peptides: Synthesis and Behavior as an Organogelator and Liquid Crystal. Beilstein Journal of Organic Chemistry, 7, 198-203. doi:10.3762/bjoc.7.26

Hudson, S. D., Jung, H. T., Percec, V., Cho, W. D., Johansson, G., Ungar, G., Balagurusamy, V. S. (1997). Direct Visualization of Individual Cylindrical and Spherical Supramolecular Dendrimers. Science, 278(5337), 449-452. doi:10.1126/science.278.5337.449

Kaucher, M. S., Peterca, M., Dulcey, A. E., Kim, A. J., Vinogradov, S. A., Hammer, D. A., Heiney, P. A., Percec, V. (2007). Selective Transport of Water Mediated by Porous Dendritic Dipeptides. Journal of American Chemical Society, 129, 11698-11699. doi:10.1021/ja076066c

Kuang, G., Jia, X., Teng, M., Chen, E., Li, W., Ji, Y. (2011). Organogels and Liquid Crystalline Properties of Amino Acid-Based Dendrons: A Systematic Study on Structure-Property Relationship. Chemistry of Materials, 24, 71-80. dx.doi.org/10.1021/cm201913p

Lee, D. R., Park, J. S., Bae, I., Lee, Y., Kim, B. M. (2016). Liquid Crystal Nanoparticle Formulation as an Oral Drug Delivery System for Liver-specific Distribution. International Journal of Nanomedicine, 8. doi:10.2147/ijn.s97000

Li, N., Guo, C., Duan, Z., Yu, L., Luo, K., Lu, J., Gu, Z. (2016). A Stimuli-responsive Janus Peptide Dendron–drug Conjugate as a Safe and Nanoscale Drug Delivery Vehicle for Breast Cancer Therapy. Journal of Materials Chemistry B, 4(21), 3760-3769. doi:10.1039/c6tb00688d

Marine, J. E., Song, S., Liang, X., Rudick, J. G. (2015). Bundle-Forming α-Helical Peptide–Dendron Hybrid. Chemical Communications, 51(76), 14314-14327. doi:10.1039/c5cc05468k.

Marine, J. E., Song, S., Liang, X., Rudick, J. G. (2016). Synthesis and Self-Assembly of Bundle-Forming α-Helical Peptide–Dendron Hybrids. Biomacromolecules, 17(1), 336-344. doi:10.1021/acs.biomac.5b01452

Mendes, A., Strohmenger, T., Goycoolea, F., Chronakis, I. (2017). Electrostatic Self-Assembly of Polysaccharides into Nanofibers. Colloids and Surfaces A: Physicochemical and Engineering Aspects, 531, 182-188. https://doi.org/10.1016/j.colsurfa.2017.07.044

Nanjwade, B. K., Bechra, H. M., Derkar, G. K., Manvi, F. V., Nanjwade, V. K. (2009) Dendrimers: Emerging Polymers for Drug-Delivery Systems. European Journal of Pharmaceutical Sciences, 38, 185-196. doi:10.1016/j.ejps.2009.07.008

O'Neill, M., Kelly, S. (2003). Liquid Crystals for Charge Transport, Luminescence, and Photonics. Advanced Materials, 15(14), 1135-1146. doi:10.1002/adma.200300009

Paineau, E., Krapf, M. M., Amara, M., Matskova, N. V., Dozov, I., Rouziere, S., Thill, A., Launois, P., Davidson, P. (2016). A Liquid-Crystalline Hexagonal Columnar Phase in Highly Dilute Suspensions of Imogolite Nanotubes. Nature Communications, doi: 10.1038/ncomms10271

Paleos, C. M., Tsiourvas, D. (2001). Supramolecular Hydrogen-bonded Liquid Crystals. Liquid Crystals, 28(8), 1127-1161. doi:10.1080/02678290110039516

Percec, V., Dulcey, A. E., Balagurusamy, V. S., Miura, Y., Smidrkal, J., Peterca, M., Vinogradov, S. A. (2004). Self-assembly of Amphiphilic Dendritic Dipeptides into Helical Pores. Nature, 430(7001), 764-768. doi:10.1038/nature02770

Percec, V., Dulcey, A. E., Peterca, M., Ilies, M., Sienkowska, M. J., Heiney, P. A. (2005). Programming the Internal Structure and Stability of Helical Pores Self-Assembled from Dendritic Dipeptides via the Protective Groups of the Peptide. Journal of the American Chemical Society, 127(50), 17902-17909. doi:10.1021/ja056313h

Percec, V., Dulcey, A. E., Peterca, M., Ilies, M., Nummelin, S., Sienkowska, M. J., Heiney, P. A. (2006). Principles of Self-Assembly of Helical Pores from Dendritic Dipeptides. PNAS, 103(8), 2518-2523. www.pnas.orgcgidoi10.1073pnas.0509676103

Percec, V., Dulcey, A. E., Peterca, M., Adelman, P., Samant, R., Balagurusamy, V. S. K., Heiney, P. A. (2007). Helical Pores Self-Assembles from Homochiral Dendritic Dipeptides Based on $_{L}$-Tyr and Nonpolar r-Amino Acids. Journal of the American Chemical Society, 129, 5992-6002. doi: 10.1021/ja071088k

Ponomarenko, S. A., Boiko, N. I., Shibaev, V. P. (2001) Liquid-Crystal Dendrimers. Polymer Science Series C, 43(1), 1-45.

Rosen, B. M., Peterca, M., Morimitsu, K., Dulcey, A. E., Leowanawat, P., Resmerita, A., Imam, M. R., Percec, V. (2011). Programming the Supramolecular Helical Polymerization of Dendritic Dipeptides via the Stereochemical Information of the Dipeptide. Journal of the American Chemical Society, 133, 5135-5151. dx.doi.org/10.1021/ja200280h

Sadler, K., Tam, J. P. (2002). Peptide Dendrimers: Applications and Synthesis. Molecular Biotechnology, 90, 195-229.

Saez, I. M., Goodby, J. W, (2005). Supermolecular Liquid Crystals. Journal of Materials Chemistry, 15, 26-40. doi: 10.1039/b413416h

Sharma, V. S., Vekariya, R. H., Sharma, A. S., Patel, R. B. (2017). Mesomorphic Properties of Liquid Crystalline Compounds with Chalconyl Central Linkage in Two Phenyl Rings. Liquid Crystals Today, 26(3), 46-54. doi: 10.1080/1358314X.2017.1359401

Tschierske, C. (2011). Fluorinated Liquid Crystals: Design of Soft Nanostructures and Increased Complexity of Self-Assembly by Perfluorinated Segments. Top Current Chemistry, 318, 1-108. doi: 10.1007/128_2011_267

Zeng, F., Zimmerman, S. C. (1997). Dendrimers in Supramolecular Chemistry: From Molecular Recognition to Self-Assembly. Chemical Reviews, 1681-1712. doi:10.1021/cr9603892